A Business Model for Multimedia Streaming in Mobile Clouds

Giovanni Schembra and Giuseppe Incarbone

***Abstract*—In the last few years, the proliferation of mobile devices coupled with the ever-increasing popularity of multimedia applications, has stimulated great interest of new figures of service providers. The major objective is to offer mobile users, located in limited areas, with broadband multimedia applications enriched with services and functionalities specific to mobile scenarios. This is the case, for example, of passengers waiting to board in an airport, visitors to a museum, or spectators at a football stadium. Since cellular networks usually cannot deliver bitrates suitable for such kinds of applications to every single user, the most appealing solution for providing mobile users with multimedia applications is to organize users into mobile clouds. In this context, this paper considers delay-constrained multimedia streaming applications over mobile clouds, and defines a business model for managing these kinds of services. Users are divided into two classes, according to the way they intend to pay for the service: in bandwidth and energy for traffic relaying (cheap-tariff) or with some money (full-tariff). An analytical model is proposed for designing the main system parameters and deciding on the tariffs of the business model. Finally, the business model is applied to a case study.**

***Index Terms*—Mobile clouds, multimedia applications, business model, Markov models, quality of service.**

I. Introduction

In the last decade mobile communications systems have registered a tremendous increasing trend to meet the user goal of communicating any information with anyone, at any time, from anywhere. This trend has been supported by both software and hardware evolution, with ever more efficient, customizable and user-friendly operating systems, and more sophisticated hardware platforms with longer battery life, versatile connecting interfaces and greater memory and CPU capabilities. Thanks to the integration of GPS, video camera and other facilities, mobile devices are really becoming mobile supercomputers for multimedia applications. With the evolution from 3G to 4G systems, the major objective is to offer mobile users with broadband multimedia applications like the ones already accessible from the current fixed network, and enriched with services and functionalities specific for mobile scenarios.

Today's most interesting mobile multimedia applications, such as Video on Demand (VoD) and IPTV, are based on distributing multimedia content to a high number of receivers simultaneously in a multipoint fashion. At the same time there is a strong increasing interest in many other multimedia multipoint applications, with specific peculiarities and requirements that make them substantially different from the previous ones. Many of them are context-specific, and involve a group of people located within proximity in a limited area. This is the case, for example, of passengers waiting for boarding in an airport, visitors in a museum, or spectators in a football stadium. In most of the above situations, users access the network with a mobile terminal, connecting the Internet through a cellular link. However, if a high number of mobile terminals use services with high bandwidth requirements, the access points to the fixed networks may not be able to satisfy user requests. Although technological advancements in wireless networks such as LTE tend to increase the maximum transmission bitrate, the average effective bitrate per user may result unsatisfactory for high quality multimedia streaming.

The most appealing solution to address this problem, to provide mobile users within proximity with multipoint applications, is to realize mobile clouds [1]. A mobile cloud is a cooperative arrangement of dynamically connected wireless nodes in close proximity to each other sharing opportunistically resources. According to this paradigm, mobile devices of the same cloud are organized in a wireless ad-hoc network to access the Internet through the cellular link shared by one or some of them, with the objective of increasing bandwidth and saving energy for mobile devices as well as for the network operators.[1] Each mobile node cooperate with the others contributing with its uploading capacity, making this approach scalable with the number of nodes.

The proposed paradigm, if compared with other systems with the same target, presents at least the two following main advantages:

1) providing multimedia streaming capability to users that are not able to directly connect to the Internet through a cellular connection, either because they have not got an active contract with a cellular operator or for problems of limited battery autonomy;

Manuscript received October 4, 2013; revised March 17, 2014; accepted May 26, 2014. Date of publication August 7, 2014; date of current version September 5, 2014. This work was partially supported by the Programma Operativo Nazionale Ricerca & Competitività 2007–2013 within the project PON04a2_E—SINERGREEN—RES NOVAE—Smart Energy Master per il governo energetico del territorio. The associate editor coordinating the review of this paper and approving it for publication was Y. Diao.

The authors are with the Dipartimento di Ingegneria Elettrica Elettronica e Informatica (DIEEI), University of Catania, Catania 95125, Italy (e-mail: giuseppe.incarbone@dieei.unict.it; schembra@dieei.unict.it).

Color versions of one or more of the figures in this paper are available online at http://ieeexplore.ieee.org.

Digital Object Identifier 10.1109/TNSM.2014.2346084

[1] Let us stress that the concept of mobile cloud is different from the concept of mobile cloud computing. In fact, as described in the paper, mobile cloud is a scheme for organizing cooperative mobile devices in wireless networks for resource sharing. Instead, mobile cloud computing [35] refers to the concept of computation offloading, which can be used for example to reduce computation time and save energy for battery powered mobile devices.

2) achieving energy saving for both cellular operators and mobile clients. In fact, from the cellular operator point of view, use of the proposed paradigm allows the operator to maintain only one cellular connection active per mobile cloud. On the other hand, from the mobile client perspective, only one client has to maintain active its cellular connection, while the others can turn-off it, using only their WiFi connection, that is less expensive in terms of energy with a factor of about four times [2], [3].

The mobile cloud paradigm is stimulating the birth of new service providers focusing on providing new multimedia services. These service providers are manifesting great interest not only for classical multimedia applications, like video streaming and video on demand, but also for new real-time interactive multipoint applications, that are more difficult to be managed because of their stringent quality of service (QoS) requirements.

Applying the mobile cloud paradigm to this kind of services seems today not sufficiently explored, and constitutes a challenging research activity in the immediate future. In fact, many problems arise in this context that are not present in other scenarios. For example, for this last kind of applications, a network mesh topology cannot be used because it may introduce an unacceptable end-to-end delay due to both a not controllable number of hops and loose of the packet delivery sequence. Moreover, the application of techniques of network coding proposed in this context [4], [5] risk to cause mobile terminal energy waste that exceeds energy saving motivating the application of these techniques.

In addition, new business models are needed to support the economical growth of these kinds of applications. To this purpose this paper defines a business model to manage delay-constrained multimedia streaming services over mobile clouds. Users are divided in two classes, according to the way they intend to pay the service: in bandwidth and energy for traffic relaying (cheap-tariff), or with some money (full-tariff).

More specifically, the following innovative key elements are introduced in the paper:

1) a *delay-constrained multimedia multipoint mobile cloud* which privileges end-to-end requirements in terms of end-to-end delay, and avoids complexities like multiple tree management, problems of out-of-order packets due to mesh overlay network topology, and high computational and memory loads due to sophisticated computation techniques (e.g., network coding) that are not suitable for mobile terminals like PDA and smart phones;
2) a *business model* for delay-constrained multimedia streaming applications over mobile clouds;
3) a *topology management strategy* for multimedia mobile clouds to support delay-sensitive applications with two classes of mobile nodes, as required by the proposed business model;
4) a *mobile node admission control (MNAC) policy* to provide active users with QoS guarantees; the idea of MNAC, inherited from the admission control concept defined in the past for service-guaranteed networks like ATM [6], is applied to accept mobile nodes until the system is able to guarantee the required level of QoS to all the active nodes;
5) an *analytical tool* to design the main network parameters and the business model variables.

The paper is structured as follows. In Section II a summary of the related work is presented. Section III describes the considered system and the proposed mobile cloud management protocols. Section IV proposes the business model for a provider of multimedia services in mobile clouds. Section V introduces an analytical Markov model of the whole system to design the main parameters and decide the tariffs of the business model. Section VI analytically derives the main performance parameters. Section VII evaluates the accuracy of the proposed model via simulation. Section VIII applies the model to achieve a numerical analysis of the behavior of the system, and characterize the business model, calculating the tariffs that maximize the service provider revenue in a case study. Finally, Section IX concludes the paper.

II. Related Work

In this section we discuss related work in the areas of multicast multimedia streaming, mobile clouds and service pricing models.

Since the introduction of the first commercial products in 1995, multicast multimedia streaming has experienced a phenomenal growth, and has stimulated considerable research efforts, particularly directed towards efficient, robust, scalable and low-latency video coding and transmission [7]. A lot of work has been done in the context of multimedia streaming in mobile ad hoc networks and infrastructure-based wireless networks, but the main focus has regarded robust encoding techniques and resource allocation [8], [9]. Sinkar *et al.* in [10] introduced a peer-to-peer (p2p) approach based on user cooperation to recover lost packets in a generic multicast service, but did not address specific multimedia services with stringent QoS requirements in terms of end-to-end delay. Then a high number of topology structures and service management protocols for multimedia contents dissemination have been proposed [11]–[13], but none of them is suitable to the context considered in this paper. Works proposing mesh [14] or forest [15]–[17] topologies require specific and complex source and channel encoding techniques [18] that are not feasible for devices with low computation capabilities and battery lifetime. Other works proposing tree topologies [19], [20] are not able to guarantee QoS for delay-constrained applications. On the contrary, in this paper we apply a tree-structured topology, but we limit the available room of the tree and introduce an admission control policy to achieve QoS guarantees.

Previous works, as for example [21], [22], proposed to use an admission control scheme to manage the access of nodes in an overlay network, but they centered their focus on security aspects, trying to match admission control mechanisms with appropriate cryptographic techniques and protocols. Instead, at the best of our knowledge, this is the first time an admission control scheme is proposed to a mobile cloud to achieve QoS requirements, expressed in terms of end-to-end delay from the source.

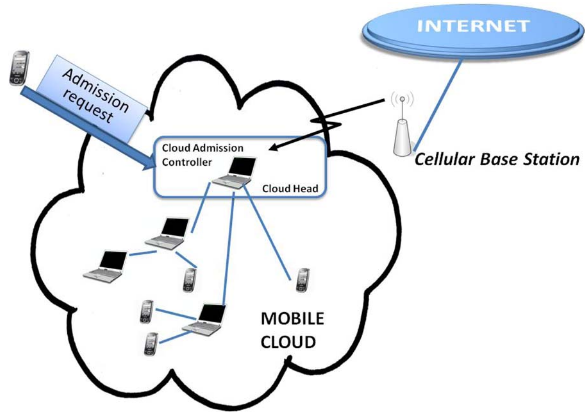

Fig. 1. Mobile cloud Internet connection sharing.

Another paper peculiarity is the application scenario, that is mobile cloud. The mobile cloud approach seems today to be an appropriate solution to increase download bandwidth to mobile users located within proximity. It is based on the concept of user cooperation. A wide discussion on the motivations leading users to cooperate to dynamically create mobile clouds can be found in [5]. A lot of research work in the recent literature was centered on the importance of the mobile cloud paradigm in terms of energy saving and new service deployments [4]. Other works aim at evaluating the capabilities of the current technologies for mobile devices and network infrastructures to support this new paradigm in terms of memory, processing power, batteries and wireless link bandwidth (see for example [23]). Some implementation solutions for content sharing applications that do not present stringent constraints in terms of end-to-end delay are appearing in the very recent literature [24], [25]. On the contrary, application of the mobile cloud approach to multimedia multipoint delay-sensitive communications services seems today not sufficiently explored, and constitutes the focus of this paper.

Finally, the presented work also relates to the large body of research efforts related to pricing network resources (e.g., see [26], [27]). To the best of the authors' knowledge there has been no prior work addressing pricing or demand regulation in multimedia mobile clouds. In addition, an analytical model is provided in this paper to set the tariffs that maximize the service provider revenue.

III. System Description

The system we consider in this paper is a multimedia mobile cloud constituted by mobile devices slowly moving in the same limited area. We assume that all mobile devices are in proximity within each other, that is, each device can be reachable with a single wireless hop from all the other mobile devices. Examples of application are transmissions of multipoint multimedia information in airports, museums, trains, football stadium and conference rooms. The system is sketched in Fig. 1. It is constituted by a set of cooperating devices connected to each other directly or in a multi-hop fashion by an overlay network of point-to-point wireless links (e.g. IEEE 802.11 Wi-Fi links), with the purpose of bandwidth increasing and energy saving for both mobile devices and cellular network operators. It is realized assigning the role of *mobile cloud head* to one of the mobile nodes that are available to connect to the Internet through a cellular link and share it with the other devices, in exchange for some incentive whose definition is out of the scope of this paper. This role can be passed among mobile nodes in a round-robin fashion.

To be able to control the end-to-end delay, each mobile cloud is realized with a tree-structured overlay network topology [15], [28] with a limit number of nodes to statistically guarantee QoS. If the number of users in the same area is greater than the maximum number that can be accommodated by a mobile cloud, users are assigned to different clouds.

According to the proposed business model, two classes of service are allowed: users subscribed to the first service class, in exchange for a lower tariff, provide the network with bandwidth resources, allowing forwarding to other nodes. Since users belonging to this class can be located as intermediate nodes in the tree topology and have children in the tree structure, we will refer to them as *fertile nodes*. Nodes of this class are devices with battery capacity sufficient to support packet forwarding to their children in the tree. Of course, the cloud head belongs to this class.

Users subscribed to the second class, on the other hand, do not provide other users with some resources, but accept a higher service price. Therefore they can only be leaves in the tree topology. For this reason they will be referred to as *sterile nodes*.

The maximum number of children that each fertile node can support, in the following indicated as F, is an important system parameter that strongly influences the topology. Since the upload bandwidth of each fertile node is divided to its F children, F is limited by the minimum bandwidth that has to be guaranteed to each node of the mobile cloud. For the sake of simplicity, in the following we will consider mobile nodes with the same transmission bandwidth on the wireless link. This case can be easily extended to remove this assumption.

Another main topology parameter, that is important to match the delay requirements, is the maximum number of levels of the tree, which impacts the maximum distance between a mobile node and the mobile cloud head. We will indicate this parameter as L. The range of L is limited by delay requirements. In fact, using statistical measures, it is possible to derive the probability density function (pdf) of the delay from the mobile cloud head to a mobile node located in the generic level l of the tree distribution topology. Therefore, given a delay threshold $\tilde{T}_s$, it is possible to evaluate the probability P_s that the delay of a generic mobile node from the mobile cloud head exceeds $\tilde{T}_s$, and the upper bound of the parameter L is chosen so that this probability P_s is below a certain threshold $\tilde{P}_s$.

Given that the considered system aims at statistically guaranteeing quality, the proposed tree management protocol needs a policy for mobile node admission. Borrowing from classical network literature [6], we will refer to it as mobile node admission control (MNAC). When a new node wants to enter the cloud, it has to issue an admission request to the *Cloud Admission Controller*. The role of cloud admission controller can be assigned to the current mobile cloud head.

When a *fertile node* requests admission, it is accepted if there is some room available in the tree. More specifically, when a fertile node makes an admission request, it will be located in the level nearest to the mobile cloud head with some room not occupied by fertile nodes. If the level nearest to the mobile cloud head which does not contain only fertile nodes is full (i.e., it contains at least one sterile node), one of the sterile nodes in this level is randomly chosen, substituted with the new fertile node, and reinserted in the best position available for sterile nodes. If no room is available to accommodate this sterile node, the request issued by the fertile node is rejected.

A *sterile node*, on the other hand, will only be inserted in the tree if there is some empty room; specifically, it will be inserted in the level closest to the mobile cloud head with some room available.

As far as node departures are concerned, management of sterile node departure is very easy, since this does not cause any tree modification. On the contrary, when a fertile node leaves the system, its sterile children and all the sub-trees whose root is a direct child of the leaving node have to be reinserted in the tree. The reinsertion process is carried out in such a way to minimize tree topology variations. Specifically, it is realized as follows:

- the sub-trees of the leaving node are inserted, one by one, starting from the deepest one, and positioning their roots following the accommodation rules illustrated so far for new fertile nodes; the structure of the sub-tree is preserved for the ones that are able to enter the tree completely;
- if this is not the case for some of them, their structure is preserved up to the last level that can be accommodated. Let us indicate this level as L_{acc}. The rest of the sub-tree is further split into sub-trees whose roots are the fertile nodes in the highest unaccommodated level, i.e., in the level $L_{acc}+1$; these sub-trees are accommodated following the rules described so far, and this procedure is repeated until all the fertile nodes are accommodated. Let us observe that, during the tree rearrangement process caused by the departure of a fertile node, all its fertile descendants will be able to find a room in the tree. In fact a fertile node cannot be accommodated in the tree only if the tree is full of fertile nodes, and this is not the case because the leaving node leaves at least one free place in the tree.
- then all the sterile nodes not accommodated in the previous step are inserted, one by one. More specifically, they are:
  - the direct sterile children of the leaving fertile node;
  - the sterile nodes preempted by the roots of the sub-trees inserted in the previous step;
  - the sterile nodes in the highest of the unaccommodated level $L_{acc}+1$ during each sub-tree insertion.

Since some time is needed to reorganize the tree after a node arrival or a node departure, some loss of information can occur. It can be avoided by using playout buffers at the destination nodes. Interested readers can refer to [29] for possible techniques to manage this matter.

The described approach can cause the rejection of some admission requests made by both fertile and sterile nodes, and service interruption for those sterile nodes descendants of a leaving fertile node which cannot be accommodated after the re-accommodation process. These QoS parameters will be considered in the following to design the mobile cloud configuration parameters L and F.

Let us point out that the presence of the Cloud Admission Controller does not constitute a bottleneck because its goal is only to coordinate the network topology. Multimedia content flows through the mobile nodes and does not constitute any load for the Controller.

IV. Service Provider Business Model

In this section we will define a business model for the Service Provider, accounting that both fertile and sterile nodes play a fundamental role for both the mobile cloud life and the Provider revenue. In fact, while sterile nodes give more direct earnings to the Provider, fertile nodes allow the network to be extended, so to accept more sterile nodes.

With all this in mind, the Service Provider revenue G can be defined as the product of the following three factors: 1) the actual mean number of fertile or sterile nodes; 2) the cost per time unit of the service; 3) the duration of the service. Therefore we have:

$$G \equiv \frac{\overline{N}_s \cdot \left(1 - P_s^{(Loss, f\to s)}\right) \cdot c_S}{\lambda_{OUT}^{(s)}} + \frac{\overline{N}_f \cdot c_F}{\lambda_{OUT}^{(f)}} \tag{1}$$

- $\overline{N}_s \cdot (1 - P_s^{(L)})$ being the actual mean number of sterile nodes present in the system, where $\overline{N}_s$ is the mean number of sterile nodes present in the system, and $(1 - P_s^{(Loss, f\to s)})$ the probability of a sterile node service is not interrupted during the topology re-accommodation process following fertile node departures;
- $\overline{N}_f$ being the mean number of fertile nodes present in the system;
- c_S and c_F being the tariffs applied to sterile and fertile nodes, respectively;
- $(\lambda_{OUT}^{(s)})^{-1}$ and $(\lambda_{OUT}^{(f)})^{-1}$ being the mean sterile and fertile node lifetimes, respectively.

In Section V we define an analytical model to provide the Service Provider with a tool to decide the tariffs c_S and c_F maximizing the overall revenue defined in (1), keeping in mind that, the higher the cost of the service, the smaller the interest in participating to the service. This concept will be discussed in deep in the following. The same model will also allow the Service Provider to design the parameters F and L, which have a strong impact on the performance statistically guaranteed to the mobile cloud users, and therefore to their grade of satisfaction and, finally, indirectly, on the Service Provider revenue.

V. System Model

In this section we define an analytical model of the multimedia mobile cloud for multicast streaming described in Section III. The target of the model is to assist cloud managers to design the main system parameters F and L, and decide the tariffs of the revenue model.

The proposed model is a continuous-time Markov chain which will be described by its infinitesimal generator matrix Q. Section V-A will introduce some notation and assumptions which are needed to derive the model. Then, in the same section, the state of the Markov chain will be defined, and some observations will be made with the aim of reducing the state space. Section V-B and C will model the two possible events determining a state change: mobile node arrival and mobile node departure, respectively. Finally, Section V-D will present the definition of the infinitesimal generator matrix, and calculate the steady-state probability array.

A. Notation, Assumptions, and State Definition

Before defining the analytical model, let us introduce some notations. Let L be the maximum number of levels in the mobile cloud tree topology, including the root level of the tree where the mobile cloud head is located. As said so far, it is a project parameter, and has to be carefully chosen given that it has an important impact on system performance. Let us assume that all mobile nodes accommodate at most F children, that is, F is the maximum number of branches for each node in the tree structure. Moreover, let us assume that the arrival and the departure processes are Poisson distributed [30]. Let $\lambda_{IN}^{(f)}$ and $\lambda_{IN}^{(s)}$ be the arrival rates for fertile and sterile nodes, and $(\lambda_{OUT}^{(f)})^{-1}$ and $(\lambda_{OUT}^{(s)})^{-1}$ be the mean sterile and fertile node lifetimes.

The Markov chain state at the generic instant t can be defined as $\underline{S}(t) = (N_1(t), \Phi_1(t), N_2(t), \Phi_2(t), \ldots, N_L(t), \Phi_L(t))$, where:

- $N_l(t)$, for each $l \in \{1, \ldots, L\}$, being the total number of mobile nodes in the generic level l at the instant t;
- $\Phi_l(t)$, for each $l \in \{1, \ldots, L\}$, being the number of *fertile nodes* in the generic level l at the instant t.

Let Y be the state space of this Markov chain. In the following we will evaluate the evolution from the generic state $\underline{s}^{(i)} = (n_1^{(i)}, f_1^{(i)}, n_2^{(i)}, f_2^{(i)}, \ldots, n_L^{(i)}, f_L^{(i)})$ to the generic state $\underline{s}^{(j)} = (n_1^{(j)}, f_1^{(j)}, n_2^{(j)}, f_2^{(j)}, \ldots, n_L^{(j)}, f_L^{(j)})$ after the following possible events: fertile and sterile node arrivals (Section V-B); fertile and sterile node departures (Section V-C).

The state space of the Markov chain may appear explosively growing with the values of L and F. However, its component variables are linked to each other and they cannot take just any value. This produces a notable state space reduction. Below we will present some rules defining the interdependence among the above component variables:

1) The number of fertile nodes in each level cannot be greater than the total number of mobile nodes in the same level, that is, $\Phi_l(t) \leq N_l(t)$, $\forall\, l \in \{1, \ldots, L\}$.
2) The number of fertile nodes in the first level of the tree is equal to 1, that is, $N_1(t) = 1$ and $\Phi_1(t) = 1$.
3) Given that only fertile nodes can have children, the total number of mobile nodes in the generic level l cannot be greater than the number of fertile nodes in the upper level, multiplied by the maximum number of children, F, that is, $N_l(t) \leq F \cdot \Phi_{l-1}(t)$, $\forall\, l \in \{2, \ldots, L\}$.

B. Mobile Node Arrival Model

Here we model the mobile node arrival event. Let us note that two possible kinds of arrivals can occur: sterile and fertile node arrivals. They can only be accepted if the conditions described in Section III are verified.

Sterile Node Arrival: As described in Section III, a new sterile node can only be accepted in the network if some room is available in the tree. Therefore, the sterile node acceptance condition is:

$$A\ sterile\ node\ is\ accepted \text{ if } \quad \exists l \text{ such that : } \quad N_l(t) < F \cdot \Phi_{l-1}(t). \tag{2}$$

In this case, the sterile node is inserted in the level $\tilde{l} = \min_l\{N_l(t) < F \cdot \Phi_{l-1}(t)\}$ and the total number of mobile nodes in the level $\tilde{l}$ increases by 1, that is, $n_{\tilde{l}}^{(j)} = n_{\tilde{l}}^{(i)} + 1$.

Fertile Node Arrival: Let us now define the fertile node acceptance condition. As we presented in Section III, an entering fertile node can be accepted in the system only if there is a fertile node with free space on its branches, or if in a level $l \neq L$ there is some sterile node to be moved down in the tree. Therefore an entering fertile node can be accepted in a level $l \in \{2, \ldots, L-1\}$ only if the number of fertile nodes in this level is less than the total number of mobile nodes that can be accommodated by the fertile nodes in the level $l-1$. Moreover, if all levels l in $\{2, \ldots, L-1\}$ are totally full of fertile nodes but the last level L of the tree is not full, the entering fertile node will be inserted in this level. So, the fertile node acceptance conditions are:

$$\begin{aligned} &A\ fertile\ node\ is\ accepted \text{ if one of the following conditions is true :}\\ &\quad a)\ \exists l \in \{2, \ldots, L-1\} \text{ such that : } \Phi_l(t) < F \cdot \Phi_{l-1}(t)\\ &\quad b)\ \Phi_l(t) = F \cdot \Phi_{l-1}(t) \quad \forall\, l \in \{1, \ldots, L-1\}\\ &\qquad\qquad \text{and } N_L(t) < F^{L-1}. \end{aligned} \tag{3}$$

When condition *a*) in (3) is true, the fertile node enters the highest level $\tilde{l}$ where the number of fertile nodes is not maximum, that is, $\tilde{l} = \min_{l \in \{1, \ldots, L-1\}}\{\Phi_l(t) < F^{l-1}\}$. If the true condition in (3) is *b*), the fertile node is inserted in the level L, that is, $\tilde{l} = L$.

To evaluate the state evolution, we have to distinguish between two different cases:

1) the entering fertile node does not preempt a sterile node, i.e. in the level $\tilde{l} - 1$ there are some mobile nodes which are able to accommodate children, that is, $N_{\tilde{l}}(t) < F^{\tilde{l}-1}$; in this case the arriving node will be inserted as a child of one of them, and therefore the state variable evolves as follows:

$$n_{\tilde{l}}^{(j)} = n_{\tilde{l}}^{(i)} + 1 \text{ and } f_{\tilde{l}}^{(j)} = f_{\tilde{l}}^{(i)} + 1 \tag{4}$$

2) in the level $\tilde{l} \in \{2, \ldots, L-1\}$ where the entering mobile node has to be accommodated there is no free room, so a sterile node has to be preempted. In this case the entering fertile node will substitute a sterile node, and the latter has to be reinserted into the tree. Let us note that, the preempted sterile node will find the new position in the tree in the level $\tilde{l} + 1$, given that the new accepted fertile

node creates room for F children. Therefore the state variable evolves as follows:

$$\begin{cases} n_{\tilde{l}}^{(j)} = n_{\tilde{l}}^{(i)} & f_{\tilde{l}}^{(j)} = f_{\tilde{l}}^{(i)} + 1 \\ n_{\tilde{l}+1}^{(j)} = n_{\tilde{l}+1}^{(i)} + 1. \end{cases} \tag{5}$$

C. Mobile Node Departure Model

Let us now model the departure of a mobile node. To this end we have to distinguish between sterile node and fertile node departures.

Sterile Node Departure: A sterile node departure can happen in the levels where some sterile node is present, i.e. where $N_l(t) > \Phi_l(t)$. So, if the leaving sterile node was in the generic level $\hat{l}$, with $n_{\hat{l}}^{(j)} > f_{\hat{l}}^{(i)}$, the state variable evolves as follows:

$$n_{\hat{l}}^{(j)} = n_{\hat{l}}^{(i)} - 1. \tag{6}$$

Fertile Node Departure: To describe the fertile node departure event we will introduce further notation to explicitly represent the tree structure. First let us note that the generic level l can accommodate at most F^{l-1} nodes, occurring in the case in which the upper level, $l-1$, is completely full with fertile nodes.

The position of a generic node in the tree can be identified by the pair (l, z), where $l \in \{1, \ldots, L\}$ represents the level of the tree occupied by the node, and $z \in \{1, \ldots, F^{l-1}\}$ its position in this level. Moreover the state of the generic position (l, z) can be represented by a ternary variable defined as follows:

$$\beta_{l,z} = \begin{cases} 0 & \text{if the position } z \text{ at the level } l \text{ is empty} \\ 1 & \text{if the position } z \text{ at the level } l \text{ contains a } sterile \text{ node} \\ 2 & \text{if the position } z \text{ at the level } l \text{ contains a } fertile \text{ node.} \end{cases} \tag{7}$$

Therefore a tree structure B with a maximum length L and a maximum number of children per node F can be exhaustively represented by the set $B = \{\beta_{l,z}\}$, for each $l \in \{1, \ldots, L\}$ and for each $z \in \{1, \ldots, F^{l-1}\}$.

Now, given a tree structure $B = \{\beta_{l,z}\}$, let us consider the sets of the positions of all nodes and all fertile nodes, respectively, which are present in the level l of B:

$$\Omega_l^{(B,All)} = \left\{(l,z) : \beta_{l,z} \neq 0, \quad \forall\, z \in \{1, \ldots, F^{l-1}\}\right\}$$

and

$$\Omega_l^{(B,Fertile)} = \left\{(l,z) : \beta_{l,z} = 2, \quad \forall\, z \in \{1, \ldots, F^{l-1}\}\right\}. \tag{8}$$

Let us indicate the number of elements in these sets as g_l and h_l, respectively. We will say that the tree structure $B = \{\beta_{l,z}\}$ is *consistent* with the state $\underline{s}^{(i)}$ if, for each level of the tree structure B, the number of fertile nodes and the total number of nodes are respectively equal to the number of fertile nodes and the total number of nodes specified by the state $\underline{s}^{(i)}$ in the same level, that is, if g_l and h_l are linked to the component l of the state variable $\underline{s}^{(i)}$ by the following relationships:

$$g_l = n_l^{(i)} \text{ and } h_l = f_l^{(i)} \quad \forall\, l \in \{1, \ldots, L\}. \tag{9}$$

Now let us define the state evolution after a mobile node departure. Let $\underline{s}^{(i)}$ be the starting state, and p be the leaving node. For each tree structure B' consistent with the starting state $\underline{s}^{(i)}$, the arrival state $\underline{s}^{(j)}$ and the number of unaccommodated sterile nodes $\alpha_{s,out}$ after both the departure of the fertile node p from the tree structure B' and the subsequent tree re-organization can be calculated as follows:

$$(s^{(j)}, \alpha_{s,out}) = \Gamma^{(F\_DEP-GLOBAL)}(p, B') \tag{10}$$

where the function $\Gamma^{(F\_DEP-GLOBAL)}(p, B')$ is derived in [31].

D. Markov Chain Definition

To define the Markov chain describing the evolution of the mobile cloud tree topology, let us calculate its infinitesimal generator, Q.

To this end, let us consider two generic states belonging to the state space Y: $\underline{s}^{(i)} = (n_1^{(i)}, f_1^{(j)}, n_2^{(i)}, f_2^{(i)}, \ldots, n_L^{(i)}, f_L^{(i)})$ and $\underline{s}^{(j)} = (n_1^{(j)}, f_1^{(j)}, n_2^{(j)}, f_2^{(j)}, \ldots, n_L^{(j)}, f_L^{(j)})$. They represent the starting and arrival states of a generic transition. The infinitesimal generator can be calculated taking into account that four possible events can modify the Markov chain state: sterile and fertile node arrivals, occurring with frequencies of $\lambda_{IN}^{(s)}$ and $\lambda_{IN}^{(f)}$, respectively, and sterile and fertile node departures, occurring with frequencies of $\lambda_{OUT}^{(s)}$ and $\lambda_{OUT}^{(f)}$, respectively. So the generic element of the infinitesimal generator is:

$$Q_{\left[\underline{s}^{(i)}, \underline{s}^{(j)}\right]} = \begin{cases} \gamma\left(\underline{s}^{(i)}, \underline{s}^{(j)}\right) & \text{if } \underline{s}^{(i)} \neq \underline{s}^{(j)} \\ -\sum\limits_{s^{(m)} \in \mathrm{Y} \setminus \left\{\underline{s}^{(i)}\right\}} Q_{\left[\underline{s}^{(i)}, s^{(m)}\right]} & \text{if } \underline{s}^{(i)} = \underline{s}^{(j)} \end{cases} \quad \text{with}$$

$$\begin{aligned} \gamma\left(\underline{s}^{(i)}, \underline{s}^{(j)}\right) &= \lambda_{IN}^{(s)} \delta_{IN}^{(s)}\left(\underline{s}^{(i)}, \underline{s}^{(j)}\right) + \lambda_{IN}^{(f)} \delta_{IN}^{(f)}\left(\underline{s}^{(i)}, \underline{s}^{(j)}\right) \\ &\quad + \lambda_{OUT}^{(s)} \delta_{OUT}^{(s)}\left(\underline{s}^{(i)}, \underline{s}^{(j)}\right) + \lambda_{OUT}^{(f)} \eta_{OUT}^{(f)}\left(\underline{s}^{(i)}, \underline{s}^{(j)}\right) \end{aligned} \tag{11}$$

where:

- $\delta_{IN}^{(s)}(\underline{s}^{(i)}, \underline{s}^{(j)})$ is the indicator function of the feasibility of a transition from the state $\underline{s}^{(i)}$ to the state $\underline{s}^{(j)}$ for a sterile node arrival. It can be defined by taking into account that an arriving sterile node is accepted in a level $\bar{l}$ if the level $\bar{l}$ is the first level where some free room is available. In this case the number of nodes in the level $\bar{l}$ is increased by one, while the number of fertile nodes remains the same. Therefore:

$$\delta_{IN}^{(s)}\left(\underline{s}^{(i)}, \underline{s}^{(j)}\right) = \begin{cases} 1 & \text{if } \exists \bar{l} : \begin{bmatrix} n_l^{(i)} = F \cdot f_{l-1}^{(i)} \quad \forall\, l < \bar{l} \\ n_{\bar{l}}^{(i)} < F \cdot f_{\bar{l}-1}^{(i)} \\ \left(n_{\bar{l}}^{(j)}, f_{\bar{l}}^{(j)}\right) = \left(n_{\bar{l}}^{(i)} + 1, f_{\bar{l}}^{(i)}\right) \end{bmatrix} \\ 0 & \text{otherwise.} \end{cases} \tag{12}$$

In the above definition, for the sake of conciseness, we have emphasized only the state variables subject to changes. The same will be done hereafter.

- $\delta_{IN}^{(f)}(\underline{s}^{(i)}, \underline{s}^{(j)})$ is the indicator function of the feasibility of a transition from the state $\underline{s}^{(i)}$ to the state $\underline{s}^{(j)}$ for a fertile node arrival. It can be defined by taking into account that an arriving fertile node is accepted in the level $\bar{l}$ in three different cases:
    A. the fertile node enters a level with some free room; this happens if the level $\bar{l}$ is the first level where some room is available;
    B. the fertile node enters the system throwing out a sterile node that can be reinserted in the tree; this happens if the accepting level $\bar{l}$ is different from L and is a full level, but it is the first level with a sterile node; in this case the sterile node is accommodated as a child of the new fertile node;

Therefore we have:

$$\delta_{IN}^{(f)}\left(\underline{s}^{(i)}, \underline{s}^{(j)}\right) = \begin{cases} 1 & \text{if } \textit{condition } A \text{ is TRUE} \\ & \text{or } \textit{condition } B \text{ is TRUE} \\ 0 & \text{otherwise} \end{cases} \tag{13}$$

where:

$$\begin{array}{l} \textit{condition } A \\ \exists\, \bar{l} \in [2, L] : \begin{bmatrix} f_l^{(i)} = F^{l-1} \quad \forall\, l < \bar{l} \\ n_{\bar{l}}^{(i)} < F^{\bar{l}-1} \\ \left(n_{\bar{l}}^{(j)}, f_{\bar{l}}^{(j)}\right) = \left(n_{\bar{l}}^{(i)} + 1, f_{\bar{l}}^{(i)} + 1\right) \end{bmatrix} \\ \textit{condition } B \\ \exists\, \bar{l} \in \{2, \ldots, L-1\} : \begin{bmatrix} f_l^{(i)} = F^{l-1} \quad \forall\, l < \bar{l} \\ n_{\bar{l}}^{(i)} = F^{\bar{l}-1} \text{ and } f_{\bar{l}}^{(i)} < F^{\bar{l}-1} \\ \left(n_{\bar{l}}^{(j)}, f_{\bar{l}}^{(j)}\right) = \left(n_{\bar{l}}^{(i)}, f_{\bar{l}}^{(i)} + 1\right) \\ \left(n_{\bar{l}+1}^{(j)}, f_{\bar{l}+1}^{(j)}\right) = \left(n_{\bar{l}+1}^{(i)} + 1, f_{\bar{l}+1}^{(i)}\right) \end{bmatrix} \end{array} \tag{14}$$

- $\delta_{OUT}^{(s)}(\underline{s}^{(i)}, \underline{s}^{(j)})$ is the indicator function of the feasibility of a transition from the state $\underline{s}^{(i)}$ to the state $\underline{s}^{(j)}$ for a sterile node departure. It can be defined by taking into account that a sterile node departure can happen in the level $\bar{l}$ if, of course, this level contains at least one sterile node. In this case the number of mobile nodes in the level $\bar{l}$ is decreased by one, while the number of fertile nodes remains the same. Therefore:

$$\delta_{OUT}^{(s)}\left(\underline{s}^{(i)}, \underline{s}^{(j)}\right) = \begin{cases} 1 \text{ if } \exists \bar{l} : & n_{\bar{l}}^{(i)} > f_{\bar{l}}^{(i)} \text{ and} \\ & \left(n_{\bar{l}}^{(j)}, f_{\bar{l}}^{(j)}\right) = \left(n_{\bar{l}}^{(i)} - 1, f_{\bar{l}}^{(i)}\right) \\ 0 & \text{otherwise} \end{cases} \tag{15}$$

- $\eta_{OUT}^{(f)}(\underline{s}^{(i)}, \underline{s}^{(j)})$ is the transition probability from $\underline{s}^{(i)}$ to $\underline{s}^{(j)}$ after a fertile node departure. To calculate $\eta_{OUT}^{(f)} \times (\underline{s}^{(i)}, \underline{s}^{(j)})$ we indicate the set of all the tree structures consistent with the states $\underline{s}^{(i)}$ and $\underline{s}^{(j)}$ as $\Lambda^{(\underline{s}^{(i)})}$ and $\Lambda^{(\underline{s}^{(j)})}$, respectively. Let $B' \in \Lambda^{(\underline{s}^{(i)})}$ and $B'' \in \Lambda^{(\underline{s}^{(j)})}$ be two structures consistent with the states $\underline{s}^{(i)}$ and $\underline{s}^{(j)}$, respectively. According to the Markov chain state aggregation theory [26], the probability of a transition from the state $\underline{s}^{(i)}$ to the state $\underline{s}^{(j)}$ can be calculated as a function of the probabilities of transition between all the tree structures consistent with $\underline{s}^{(i)}$ and $\underline{s}^{(j)}$ as follows:

$$\eta_{OUT}^{(f)}\left(\underline{s}^{(i)}, \underline{s}^{(j)}\right) = \sum_{B' \in \Lambda\left(\underline{s}^{(i)}\right)} \text{Prob}\left\{B' \to \underline{s}^{(j)}\right\} \cdot \nu_{[B' | \underline{s}^{(i)}]} \quad \forall\, \underline{s}^{(i)},\ \underline{s}^{(j)} \in \mathrm{Y} \tag{16}$$

1) $\text{Prob}\{B' \to \underline{s}^{(j)}\}$ being the probability of transition from the tree structure B' to any tree structure consistent with $\underline{s}^{(j)}$, after a mobile node departure;
2) $\nu_{[B'|\underline{s}^{(i)}]}$ being the conditional probability that the tree structure is B', provided that it is in the state $\underline{s}^{(i)}$. Given that all the specific tree structures in the same state $\underline{s}^{(i)}$ have the same probability, we have:

$$\nu_{[B' | \underline{s}^{(i)}]} = \frac{1}{N^{(\underline{s}^{(i)})}} \tag{17}$$

where $N^{(\underline{s}^{(i)})}$ is the number of tree structures consistent with the state $\underline{s}^{(i)}$.

Finally, indicating the set of fertile nodes in the tree structure B' as $\Psi^{(B', Fertile)}$, and applying the theorem of total probability over all the possible fertile nodes that can leave the tree, we have:

$$\begin{aligned} &\eta_{OUT}^{(f)}\left(\underline{s}^{(i)}, \underline{s}^{(j)}\right) \\ &= \sum_{B' \in \Lambda\left(\underline{s}^{(i)}\right)} \sum_{p \in \Psi^{(B', Fertile)}} \text{Prob}\left\{p \text{ leaves the tree, } B' \to \underline{s}^{(j)}\right\} \\ &\quad \cdot \nu_{[B' | \underline{s}^{(i)}]} \\ &= \sum_{B' \in \Lambda\left(\underline{s}^{(i)}\right)} \sum_{p \in \Psi^{(B', Fertile)}} \text{Prob}\left\{B' \to \underline{s}^{(j)} \middle| p \text{ leaves the tree}\right\} \\ &\quad \cdot \text{Prob}\{p \text{ leaves the tree} | B'\} \cdot \nu_{[B' | \underline{s}^{(i)}]} \end{aligned} \tag{18}$$

where $\text{Prob}\{p \text{ leaves the tree}|B'\}$ is the probability that the generic mobile node p leaves the tree when the tree structure is B'. Let us note that this probability only depends on the number of fertile nodes in the tree, and not on the particular tree structure; therefore we have:

$$\text{Prob}\{p \text{ leaves the tree} | B'\} = 1 \Bigg/ \sum_{l=2}^{L} f_l^{(i)}. \tag{19}$$

Let us note that the term $\text{Prob}\{B' \to s^{(j)} | p \text{ leaves the tree}\}$ is a Boolean function which is true only if, after the departure of the mobile node p when the tree structure is B', the new tree structure is consistent with the state $\underline{s}^{(j)}$. Therefore it can be calculated as follows:

$$\text{Prob}\left\{B' \to \underline{s}^{(j)} \middle| p \text{ leaves the tree}\right\} = \begin{cases} 1 & \text{if } \hat{\underline{s}} = \underline{s}^{(j)} \\ 0 & \text{if } \hat{\underline{s}} \neq \underline{s}^{(j)} \end{cases} \tag{20}$$

where $\hat{\underline{s}}$ is the result of the function $\Gamma^{(F\_DEP-GLOBAL)}(p, B')$ described in [31], as the arrival state reached starting from the tree structure B' when the mobile node p leaves the tree.

Once the matrix Q has been derived, the system steady-state probability array, whose generic element is $\pi_{[\underline{s}]} = \text{Prob}\{\underline{S}(t) = \underline{s}\}$, can be calculated as the solution of the following linear system $\underline{\pi} \cdot Q = \underline{0}$, with the condition that the sum of all the elements of $\pi_{[\underline{s}]}$ is equal to 1.

VI. Performance Analysis

In this section we use the steady-state probability array derived in the previous section to evaluate the main performance indices of the mobile cloud being considered. According to the previous notation, let us indicate the generic state of the system as $\underline{s} = (n_1, f_1, \ldots, n_L, f_L)$ and its state probability as $\pi_{[\underline{s}]}$. More specifically, in the following we will evaluate the main QoS parameters regarding the number of mobile nodes in the cloud (Section VI-A), the mobile node rejection probability and the sterile node interruption probability due to the departure of a fertile node (Section VI-B), and the delay from the mobile cloud head (Section VI-C).

A. Number of Mobile Nodes in the Network

The first parameters we evaluate regard the number of mobile nodes present in the mobile cloud besides the mobile cloud head, at a generic instant, considering all of them, fertile and sterile, separately. Specifically, the probability density function (pdf) of the total number of mobile nodes in the cloud can be evaluated as follows:

$$\varphi_{N_{All}}(\rho) = \text{Prob}\{\rho \text{ peers}\} = \sum_{\underline{s}\in \Upsilon} \pi[\underline{s}] \cdot \delta_\rho^{(All)}(\underline{s})$$
$$\text{where } \delta_\rho^{(All)}(\underline{s}) = \begin{cases} 1 & \text{if } \sum_{l=2}^{L} n_l = \rho \\ 0 & \text{otherwise.} \end{cases} \tag{21}$$

The function $\delta_\rho^{(All)}(\underline{s})$ is the indicator function of the states where the total number of mobile nodes is equal to ρ. The pdfs of the number of fertile and sterile nodes can be calculated likewise:

$$\varphi_{N_f}(\rho) = \text{Prob}\{\rho \text{ fertile peers}\} = \sum_{\underline{s}\in \Upsilon} \pi[\underline{s}] \cdot \delta_\rho^{(f)}(\underline{s})$$
$$\varphi_{N_s}(\rho) = \text{Prob}\{\rho \text{ sterile peers}\} = \sum_{\underline{s}\in \Upsilon} \pi[\underline{s}] \cdot \delta_\rho^{(s)}(\underline{s}) \tag{22}$$

where $\delta_\rho^{(f)}(\underline{s})$ and $\delta_\rho^{(s)}(\underline{s})$ are defined as follows:

$$\delta_\rho^{(f)}(\underline{s}) = \begin{cases} 1 & \text{if } \sum_{l=2}^{L} f_l = \rho \\ 0 & \text{otherwise} \end{cases} \text{ and}$$
$$\delta_\rho^{(s)}(\underline{s}) = \begin{cases} 1 & \text{if } \sum_{l=2}^{L} (n_l - f_l) = \rho \\ 0 & \text{otherwise.} \end{cases} \tag{23}$$

The pdfs derived in (21) and (22) can be used to calculate the mean values of the number of fertile and sterile nodes in the cloud.

B. Mobile Node Rejection and Interruption Probabilities

Another important set of performance parameters regards mobile node admission control policy. In fact, as described in Section III, the tree management mechanism has been defined so as to guarantee a limit to the distance from the mobile cloud head. However, for this reason, loss of mobile nodes is possible. So we calculate the following probabilities:

- Fertile node admission rejection probability, $P_f^{(\text{Rej})}$
- Sterile node admission rejection probability, $P_s^{(\text{Rej})}$
- Sterile node interruption probability, due to a fertile node departure, $P_s^{(L)}$

Using the Poisson Arrivals See Time Averages (PASTA) property of Poisson processes [32], they can be calculated as follows:

$$P_f^{(\text{Rej})} = \sum_{\underline{s}\in S^{(Full)}} \pi_{[\underline{s}]} \quad P_s^{(\text{Rej})} = \sum_{\underline{s}\in S^{(\text{Rej}_S)}} \pi_{[\underline{s}]}$$
$$P_s^{(L)} = \sum_{\underline{s}\in S^{(Loss, f\to s)}} \pi_{[\underline{s}]} \tag{24}$$

where:

- $\underline{S}^{(Full)}$ is the set of states where all the room in the levels $\{1, \ldots, L-1\}$ is occupied by fertile nodes, and the last level is completely occupied by either fertile or sterile nodes; this state is characterized by $n_l = f_l = F^{l-1}$, for each $l \in \{1, \ldots, L-1\}$ and $n_L = F^{L-1}$;
- $S^{(\text{Rej}_S)}$ is the set of states where no room is available for sterile nodes, that is, the number of nodes (both sterile and fertile) in any level is equal to the maximum number of nodes that can be accommodated. Therefore, we have $S^{(\text{Rej}_S)} = \{\underline{s} : n_l = F \cdot f_{l-1} \, \forall \, l \in \{2, \ldots, L\}\}$.
- $S^{(Loss, f\to s)}$ is the set of states where a sterile node cannot be reinserted in the tree after a fertile node departure.

C. Mobile Node Position in the Tree and Delay Statistics

In this section we derive another important set of parameters regarding the position of each mobile node in the tree, with the aim of providing an estimation of the delay between the mobile cloud head and each mobile node. To this end first we will derive the probability distribution of the position occupied by a generic fertile node, here indicated as target fertile node (TFN). More specifically, the pdf of its position is:

$$\varphi_f^{(Pos)}(l') = \text{Prob}\{\text{TFN is at level } l' | N_f \neq 0\}$$
$$= \frac{\sum_{\underline{s}\in \Upsilon} \text{Prob}\{\text{TFN is at level } l' | \underline{S}(t) = \underline{s}\} \cdot \pi_{[\underline{s}]}}{1 - \text{Prob}\{N_f = 0\}} \tag{25}$$

where l' represents the level occupied by TFN, and N_f represents the number of fertile nodes in the tree. We consider the case $l' \in \{2, \ldots, L\}$ because we are analyzing the distance from the node in the first level of the tree.

The term Prob$\{$TFN is at level$l'|\underline{S}(t) = \underline{s}\}$ can be calculated as the number of fertile nodes in the level l' over the total number of fertile nodes, that is:

$$\text{Prob}\{\text{TFN is at level } l'\,|\underline{S}(t) = \underline{s}\} = \begin{cases} f_{l'} \Big/ \sum_{l=2}^{L} f_l & \text{if } \sum_{l=2}^{L} f_l \neq 0 \\ 0 & \text{otherwise.} \end{cases} \quad (26)$$

Likewise, the pdf of the position occupied by a generic sterile node, here indicated as target sterile node (TSN), is:

$$\varphi_s^{(Pos)}(l') = \text{Prob}\{\text{TSN is at level } l'|N_s \neq 0\} = \frac{\sum_{\underline{s}\in Y} \text{Prob}\{\text{TSN is at level } l'|\underline{S}(t)=\underline{s}\} \cdot \pi_{[\underline{s}]}}{1-\text{Prob}\{N_s=0\}} \quad (27)$$

where the term Prob$\{$TSN is at level $l'|\underline{S}(t) = \underline{s}\}$ can be calculated as follows:

$$\text{Prob}\{\text{TSN is at level } l'|\underline{S}(t) = \underline{s}\} = \frac{n_{l'} - f_{l'}}{\sum_{l=2}^{L}(n_l - f_l).} \quad (28)$$

The terms Prob$\{N_f = 0\}$ in (25) and Prob$\{N_s = 0\}$ in (27) can be calculated from the pdfs in (22), using $\rho = 0$.

Finally, using $\varphi_f^{(Pos)}(l')$ and $\varphi_s^{(Pos)}(l')$, we can calculate the pdf of the delay of a fertile or sterile node from the mobile cloud head:

$$f_{fertile\_peer}(t) = \sum_{l'=2}^{L} f_{l'}(t) \cdot \varphi_f^{(Pos)}(l')$$

$$f_{sterile\_peer}(t) = \sum_{l'=2}^{L} f_{l'}(t) \cdot \varphi_s^{(Pos)}(l') \quad (29)$$

where $f_{l'}(t)$ is the pdf of the delay from the tree root of a mobile node in the generic level $l' \in \{2, \ldots, L\}$. If $f_{one\_link}(t)$ is the pdf of the delay between two directly connected mobile nodes considering both the delay suffered by the transmission buffer of the sender node and the propagation delay between the sender and the receiver node (assumed as a problem input), $f_{l'}(t)$, in the generic level $l' \in \{3, \ldots, L\}$, can be calculated as:

$$f_{l'}(t) = \begin{cases} f_{one\_link}(t) & l' = 2 \\ f_{l'-1}(t) * f_{one\_link}(t) & l' \in \{3, \ldots, L\}. \end{cases} \quad (30)$$

VII. Model Accuracy Evaluation

Let us evaluate the accuracy of the proposed model. To this aim we implemented an event-driven simulator of our protocol and compared the pdfs calculated by the analytical model against the ones obtained with the simulator. To use real data patterns, we launched our simulations with real arrival and departure traces captured observing the behavior of people using smart phones in some areas of the Fiumicino—Leonardo da Vinci Airport in Rome. The average values of the above traces, $\lambda_{IN} = 12$ arr/min and $(\lambda_{OUT})^{-1} = 5$ min, were used as input parameters in the analytical model for comparison with simulation.

The comparison is done using a QQplot. For the sake of brevity in Fig. 2 we show the model accuracy results for the most representative system parameter, the number of mobile nodes in the network, considering the following network parameters: $F = 4$ and $L = 4$. The model accuracy was also tested with a different people behavior trace, with $\lambda_{IN} = 3$ arr/min and with the same mobile node value of $(\lambda_{OUT})^{-1}$ as in the previous case, and for other two values of F: $F = 2$ and $F = 3$. The results of these further tests were reported in [31]. It is important to stress that the model has been demonstrated to be accurate in capturing statistics of all the other model variables.

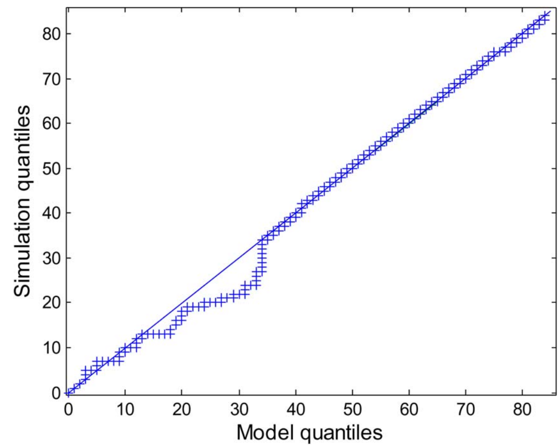

Fig. 2. QQplot of the pdf of the number of mobile cloud nodes.

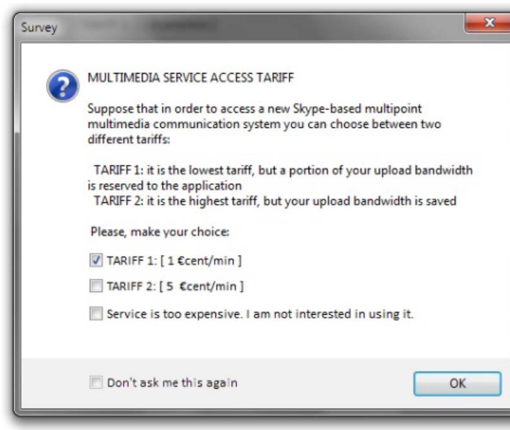

Fig. 3. Popup used in the survey.

VIII. Numerical Results

In this section we evaluate the mobile cloud performance using the analytical model presented so far, and apply the model to derive the mobile node tariffs that maximize the service provider revenue. To this end we carried out a survey (Fig. 3 shows the popup we have used to propose the survey) in a community of 3000 mobile users of Skype, chosen as a representative example of a real-time multimedia application. The

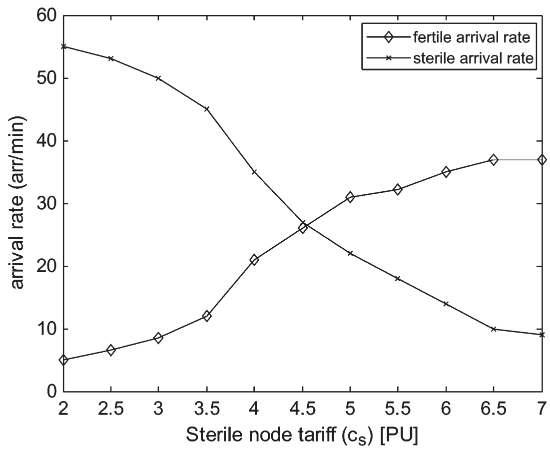

Fig. 4. Arrival rates estimated through the survey.

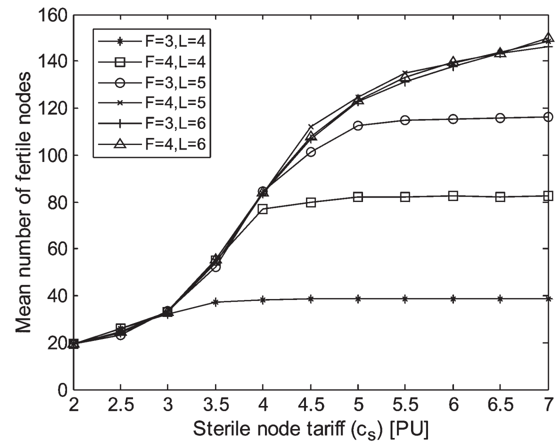

Fig. 5. Mean number of fertile nodes vs. the sterile node tariff c_s, for $c_f = 1$.

TABLE I
MOBILE CLOUD CAPACITY VS. L AND F

C	$L = 4$	$L = 5$	$L = 6$
$F = 3$	39	120	363
$F = 4$	84	346	1364

representative sample was composed by students or workers belonging to the SME (Small and Medium Enterprise) sector. More specifically we asked every community member entering the service to express his preference between three possible conditions:

- paying a cheap tariff, c_f, but providing bandwidth to the system (access the system as a fertile node);
- paying a full tariff $c_s > c_f$, but providing no bandwidth to the system (access the system as a sterile node);
- renouncing to join the service.

The values c_f and c_s express the tariffs of the service in price units for fertile and sterile nodes, respectively. For example, in our survey we used a price unit (PU) of 1 euros cent/min. The survey was repeated several times. Each time, one week long, we proposed the same value of $c_f (c_f = 1 \text{ PU})$ and different values of $c_s (c_s \in \{2, \ldots, 7\} \text{ PU})$. At the end of the survey we obtained an estimation of the mean fertile and sterile node arrival rates, $\lambda_{IN}^{(f)}$ and $\lambda_{IN}^{(s)}$, as the ratio between the number of users accepting to enter the system respectively as fertile or sterile nodes, and the duration of the survey. The results of the survey are shown in Fig. 4 against the sterile node tariff c_s.

Now we present a performance analysis, obtained by using the model proposed so far. In our analysis we consider the fertile and sterile node arrival rates $\lambda_{IN}^{(f)}$ and $\lambda_{IN}^{(s)}$ derived from Fig. 4 for each value of the sterile node tariff c_s, and $c_f = 1$. The fertile and sterile node departure rates are $\lambda_{OUT}^{(f)} = \lambda_{OUT}^{(s)} = 0.25$ departures/min.

Our first target is to evaluate the impact of the network parameters F and L. They determine the so-called *mobile cloud capacity*, defined as the maximum number of mobile nodes, besides the mobile cloud head, that the network can accommodate simultaneously. Its value is given by $C = \sum_{l=2}^{L} F^{l-1}$ (see Table I).

As discussed in Section III, the parameter F cannot assume too high values because determines the forwarding bandwidth to each children in the topology tree, that is calculated as the total uplink bandwidth given by the WiFi interface divided by F. The other important parameter that can be used to increase the cloud capacity is L. Let us note that L cannot be increased too much as well because high values of L could produce high values of the delay from the mobile cloud head in the deepest levels of the tree.

Keeping in mind these remarks, in our analysis we considered two different values of F ($F = 3$ and $F = 4$) and three different values of L ($L = 4$, $L = 5$ and $L = 6$). Table I summarizes the values of the mobile cloud capacity C in the considered scenarios.

Fig. 5 represents the mean number of fertile nodes calculated from the pdfs defined in (21) and (22) for the considered values of F and L. In this figure we notice an increase of the mean number of fertile nodes when c_s increases, and this behavior is more evident in the middle range of c_s, and for higher values of the mobile cloud capacity. This is due to the fact that, according to Fig. 4, the fertile arrival rate $\lambda_{IN}^{(f)}$ increases when the sterile node tariff c_s increases because, for high values of c_s, most of the mobile nodes prefer to enter the system as fertile node, paying more in bandwidth than in money. In addition let us note that, when the mobile cloud capacity is low, i.e. in the cases $L = 4$ and $F = 3$, $L = 4$ and $F = 4$, $L = 5$ and $F = 3$, the mean number of fertile nodes becomes almost flat; in these cases, in fact, for high values of $\lambda_{IN}^{(f)}$, the tree tends to be often full, that is, the number of fertile nodes is very close to its maximum value, coinciding with the mobile cloud capacity.

The mean number of sterile nodes vs. c_s is shown in Fig. 6. It confirms that the system behaves in two different ways according to the mobile cloud capacity. More specifically this parameter presents a prevalently monotonic decreasing trend only for low values of the mobile cloud capacity. In these cases, in fact, the tree saturates even for low values of the fertile node arrival rate, and the admission of sterile nodes when fertile node arrival rate increases, becomes rare; therefore the mean number of these mobile nodes decreases when c_s, and therefore $\lambda_{IN}^{(f)}$, increases.

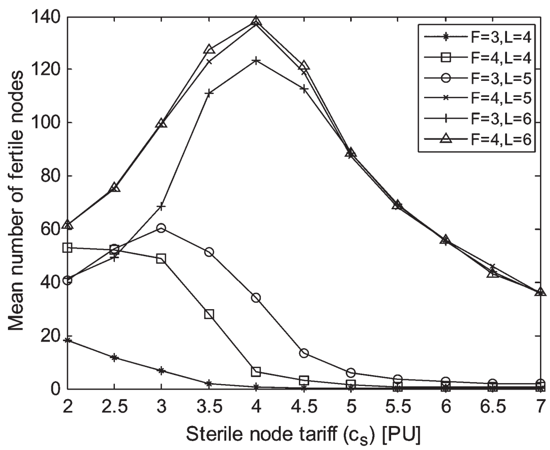

Fig. 6. Mean number of sterile nodes vs. the sterile node tariff c_s, for $c_f = 1$.

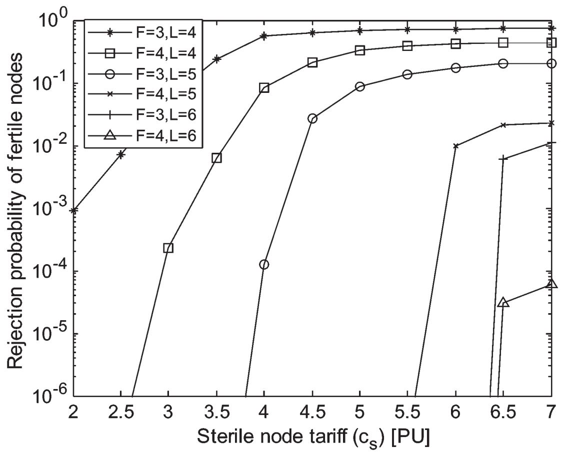

Fig. 7. Rejection probability of fertile nodes vs. the sterile node tariff c_s, for $c_f = 1$.

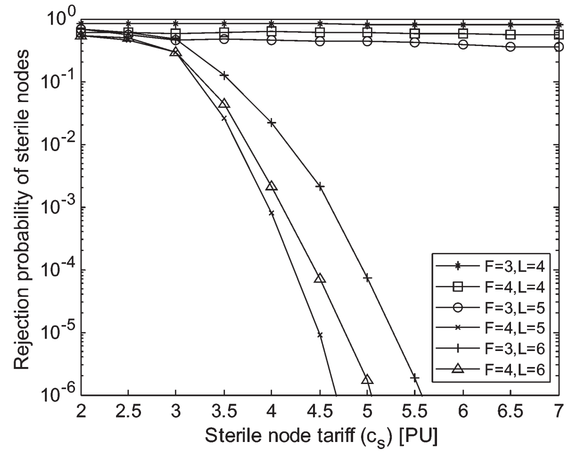

Fig. 8. Rejection probability of sterile nodes vs. the sterile node tariff c_s, for $c_f = 1$.

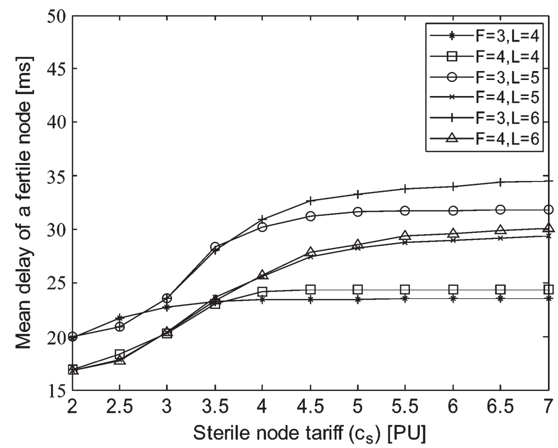

Fig. 9. Mean end-to-end delay for fertile nodes vs. the sterile node tariff c_s, for $c_f = 1$.

Let us now consider the curves in Fig. 6 for high values of the mobile cloud capacity. In these cases the mean number of sterile nodes presents a non-monotonic trend. More specifically, when the tree is not saturated by fertile nodes (i.e. for low values of c_s), an increase of the number of fertile nodes provides the network with more resources, increasing the possibility of sterile nodes being accepted. The decreasing trend for high values of c_s, on the contrary, is obvious and is due to the tree saturation when the fertile node arrival rate becomes high (as discussed in the cases of low mobile cloud capacity).

Fig. 7 presents the admission rejection probability for an entering fertile node. As we can see from this figure, this probability grows when c_s (and therefore the fertile node arrival rate) grows, being acceptable for fertile node arrival rates belonging to the low- and medium-load conditions; the same probability is very close to the unity when the system is overloaded. The figure also shows that, as expected, the fertile node admission rejection probability decreases with the increase of the mobile cloud capacity. This figure highlights the work of the proposed mobile node admission control mechanism, that has in charge to maintain the system behavior stable to allow real-time interactions, guaranteeing required performance to the accepted nodes.

Fig. 8 presents the rejection probability for sterile nodes. As we can see from the figure, the behavior of the admission rejection probability for low and high values of the mobile cloud capacity are very different from each other. More specifically, for low values of the mobile cloud capacity, the system rarely accepts sterile nodes, independently of the values of c_s, due to the network saturation by fertile nodes. On the contrary, for high values of the mobile cloud capacity, the network is not saturated by fertile nodes and the sterile node admission rejection probability decreases with the increase of the fertile node arrival rate due to the increase of c_s.

Figs. 9 and 10 present the mean delay of a generic fertile node and sterile node from the cluster head, calculated from the pdfs in (29), using an experimentally-measured one-link pdf $f_{one\_link}(t)$ with a mean value of 9 ms. As we can see, the mean delay increases when the sterile node tariff increases because a higher value of c_s determines that the number of fertile nodes in the network increases; therefore the network availability for new entering sterile or fertile nodes grows and the depth of the distribution tree increases. Moreover, from the above figures we observe that, as expected, fertile nodes have a lower delay from the cluster head than sterile nodes.

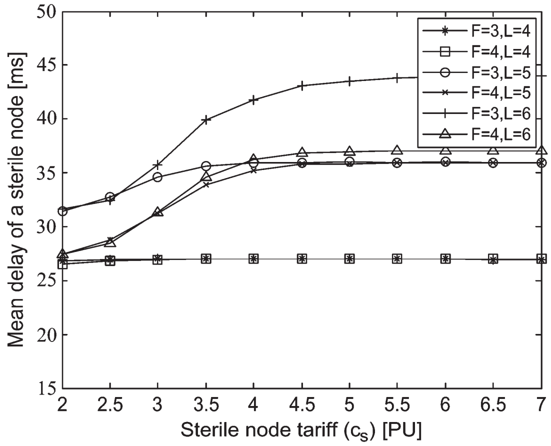

Fig. 10. Mean end-to-end delay for sterile nodes vs. the sterile node tariff c_s, for $c_f = 1$.

Now, to evaluate what happens at each fertile node departure, let us consider that this event can cause a topology modification of the mobile cloud and, consequently, all the sub-trees having the leaving node as their root need to be re-allocated. More specifically, the following matters have to be accounted:

1) the current topology, and specifically its portion constituted by the sub-trees of the leaving node, has to be modified according to the policy specified in Section III;
2) a new parent has to be assigned and communicated to some of the mobile clients, in particular to the roots of the sub-trees to be re-allocated;
3) nodes that change their level in the tree suffer a delay discontinuity that can influence perceived performance.

As described in Section III, the algorithm implemented to calculate the new topology is run by the Cloud Admission Controller in a centralized manner, and is very easy. For this reason neither system performance nor energy consumption are influenced by its run. As regards the communication of the new parent to the roots of the sub-trees to be re-allocated, since they are not many, the overhead introduced by the communication messages and the time needed to realize this communication are negligible.

The only matter that has to be considered because influencing system performance is the delay discontinuity suffered by the nodes that are located at a different level in the new topology. Although the policy of topology variation after a node departure aims at minimizing this effect, some nodes can suffer performance degradation due to this matter. To quantify it, in Figs. 11 and 12 we have represented the probability distribution of the level jump for the cases $F = 3$ and $F = 4$, defined as the difference between the levels occupied after and before a topology variation. For example, a level jump equal to 1 means that the new position of the node is in a level that is below the one occupied before the topology variation. On the contrary, a level jump of -1 means that the node has been moved up of one level. Of course, a level jump equal to 0 means that the level of the mobile node has not been changed during the topology variation. From this figure we can deduce that the most topology variations cause a level jump not greater than 1 level, that is only one hop in wireless network topology, i.e. a mean delay variation of 9 ms in our case. The relative delay discontinuity can be easily compensated by a delay jitter compensation buffer [33] that, if combined with an adaptive media playout [34], can further reduce performance degradation.

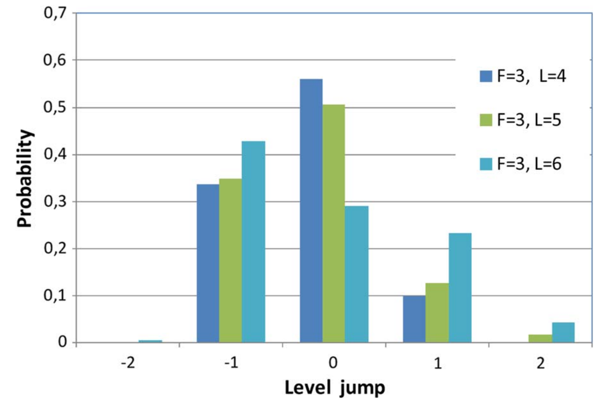

Fig. 11. Level jump probability after a fertile node departure for $F = 3$.

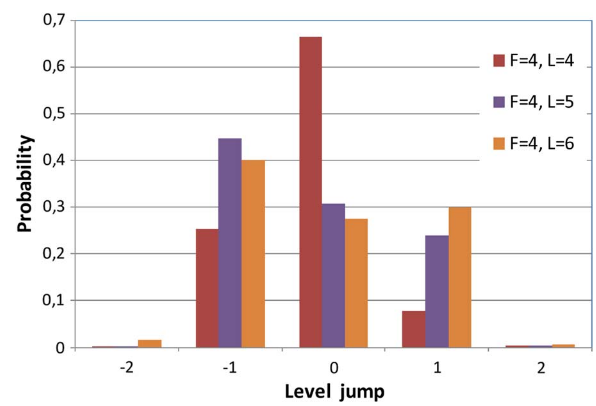

Fig. 12. Level jump probability after a fertile node departure for $F = 4$.

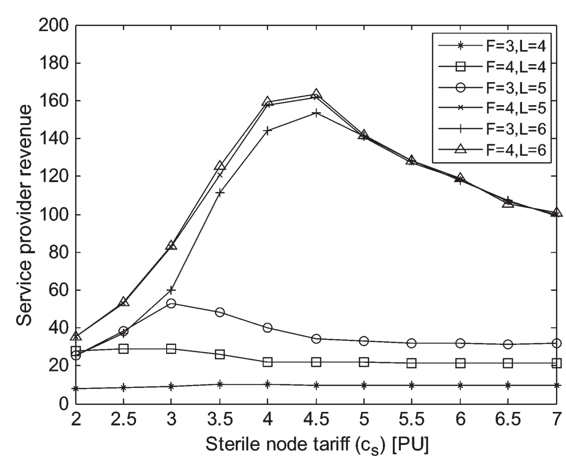

Fig. 13. Service provider revenue vs. the sterile node tariff c_s, for $c_f = 1$.

Finally, Fig. 13 shows the service provider revenue obtained according to (1), vs. the considered values of the sterile node tariff c_s. As we can see, as expected, the service provider revenue increases with the increase of the mobile cloud capacity (i.e. with an increase of F and L).

Moreover, let us note that the service provider revenue does not have a monotonic behavior, and this motivates the application of the analytical tool proposed in this paper: the curve presents a peak for intermediate values of c_s, which constitute the best tariff to be applied to the sterile nodes. The peak is more evident for higher values of the mobile cloud capacity. In fact, when the mobile cloud capacity is low, the network is always full of fertile nodes for all the values of c_s; therefore the service provider revenue does not change when the fertile and sterile node arrival rates change due to an increase of c_s. On the contrary, when the mobile cloud capacity is high, the high number of sterile nodes which can be accepted in the network makes the provider revenue highly sensitive to the applied tariffs.

From the same Fig. 13, in the case of fertile and sterile node arrival rates deduced by the survey and shown in Fig. 4, we can derive an important result for the tariff choice: when the mobile cloud capacity is sufficient to make system saturation negligible, the service provider revenue is maximized with a value of sterile node tariff equal to $c_s = 4.5$.

The proposed model can be used to decide the two main important system parameters F and L, and the tariffs to be applied to the service users that maximize the service provider revenue while respecting a given set of thresholds on performance parameters like the rejection probability, the mean delay and the minimum end-to-end transmission bandwidth. The last parameter limits the value of F since it is given by C/F, where C is the littlest WiFi link transmission bandwidth among all the mobile nodes. More specifically, the following steps can be followed:

STEP 1: Calculate the rejection probability for each considered value of node tariff, obtaining results like the ones shown in Figs. 7 and 8. Taking into account that the rejection probability

- for both fertile and sterile nodes monotonically decreases against the mobile cloud network capacity, i.e. against the values of F and L;
- for fertile nodes increases with the sterile node tariff c_s;
- for sterile nodes decreases with the sterile node tariff c_s,

it is easy to determine the boundaries of the region of parameters (F, L, c_s) where the rejection probability threshold is respected.

STEP 2: Calculate the mean delay for each considered value of node tariff, obtaining results like the ones shown in Figs. 9 and 10. Taking into account that the mean delay:

- increases against c_s;
- increases against L and decreases against F for c_s greater than a given value, while behaves in the opposite way for c_s below the above value,

it is easy to determine the boundaries of the region of parameters (F, L, c_s), subset of the region calculated at the step 1, where the mean delay respects the given threshold.

STEP 3: Calculate the service provider revenue for each considered value of node tariff, obtaining results like the ones shown in Fig. 14. Taking into account that the revenue monotonically increases with the network capacity, it is easy to find the set of parameters (F, L, c_s) as subset of the result obtained in step 2, that maximizes the revenue.

TABLE II
SET OF PARAMETERS CALCULATED AT EACH STEP OF THE SYSTEM DESIGN ALGORITHM

	Sets of parameters verifying QoS requirements		
STEP 1	$F = 4$	$L = 5$	$3.8 \le c_s \le 5.6$
	$F = 3$	$L = 6$	$3.8 \le c_s \le 5.6$
	$F = 4$	$L = 6$	$3.8 \le c_s \le 5.6$
STEP 2	$F = 4$	$L = 5$	$c_s \ge 4.6$
STEP 3	$F = 4$	$L = 5$	$c_s = 4$

For example, assume that the performance requirements are:

- Rejection probability less than $2 \cdot 10^{-3}$;
- Mean delay less than 35 ms;
- End-to-end transmission bandwidth greater than 5 Mbit/s.

Assuming that the minimum WiFi link transmission bandwidth is of $C = 21$ Mbit/s, the third requirement is verified only for $F \le 4$. Running the above algorithm we obtain the sets listed in Table II, and therefore the best set of parameters that maximizes the revenue while respecting the above requirements is the output of the step 3, that is: $F = 4$, $L = 5$ and $c_s = 4$.

Of course the presented case is just an example. However, applying the model at the same way but in different cases allows Service Providers to decide their business model and network parameters that maximize their revenue.

IX. CONCLUSION AND FUTURE WORK

This paper proposes a business model to be applied to delay-constrained multimedia applications in mobile clouds. To decide the main parameters of the business model and the main design parameters of the mobile cloud network, an analytical model has been introduced.

The first planned extension of this work is to improve the fertile node admission policy to account their transmission bandwidth, to assign a higher level to nodes with more transmission capacity. As a consequence the business model has to be modified to apply a tariff depending on the amount of transmission bandwidth provided by the mobile nodes.

Another possible extension of our work is to manage more than one mobile cloud, in such a way that mobile devices not accepted by one cloud or rejected by it can be moved to another cloud in the same area.

Another extension is to consider mobile clouds with more than one heads. In this way, if the multimedia streaming source encodes the stream with a multiple description coding (MDC) technique, it is possible to create a forest-like topology, where each tree is used to deliver one description [16], [27]. In this case the analytical model can be also used to decide the number of mobile cloud heads that guarantee an acceptable grade of perceived quality.

Finally, another possible evolution of this work can consist in considering a pricing policy based on the perceived quality of the multimedia flow. This will result very interesting in the case of MDC flows, since perceived quality depends on the number of descriptions received by each mobile device.

ACKNOWLEDGMENT

The authors would like to thank the anonymous reviewers for their valuable comments which improved the quality of this paper and clarified many important points to the reader.

REFERENCES

[1] L. Militano, F. H. P. Fitzek, A. Iera, and A. Molinaro, “On the beneficial effects of cooperative wireless peer to peer networking,” in *Proc. TIWDC*, Naples, Italy, Sep. 9–12, 2007, pp. 97–109.

[2] F. H. P. Fitzek, F. Heide, and M. V. Pedersen, “On the need of network coding for mobile clouds,” in *Proc. Autom. Appl. Comput. Sci. Workshop*, Budapest, Hungary, Jun. 24–26, 2011. [Online]. Available: http://vbn.aau.dk/files/53358555/aacs_paper.pdf

[3] J. Huang *et al.*, “A close examination of performance and power characteristics of 4G LTE networks,” in *Proc. ACM Mobisys*, Low Wood Bay, U.K., Jun. 2012, pp. 225–238.

[4] F. H. P. Fitzek and M. D. Katz, *Mobile Clouds: Exploiting Distributed Resources in Wireless, Mobile and Social Networks*. Hoboken, NJ, USA: Wiley, Feb. 2014.

[5] M. V. Pedersen and F. H. P. Fitzek, “Mobile clouds: The new content distribution platform,” *Proc. IEEE*, vol. 100, pp. 1400–1403, May 2012.

[6] R. Handel, H. Manfred, and S. Schroder, *ATM Networks: Concepts, Protocols, Applications*. Reading, MA, USA: Addison-Wesley, 1994.

[7] “Introduction to the special issue on streaming video,” *IEEE Trans. Circuits Syst. Video Technol.*, vol. 11, no. 3, pp. 265–268, Mar. 2001.

[8] S. Deb, S. Jaiswal, and K. Nagaraj, “Real-time video multicast in WiMAX networks,” in *Proc. IEEE INFOCOM*, Phoenix, AZ, USA, Apr. 15–17, 2008, pp. 2252–2260.

[9] D. Hu, S. Mao, and J. H. Reed, “On video multicast in cognitive radio networks,” in *Proc. IEEE INFOCOM*, Rio de Janeiro, Brazil, Apr. 2009, pp. 2222–2230.

[10] K. Sinkar *et al.*, “Cooperative recovery in heterogeneous mobile networks,” in *Proc. IEEE SECON*, San Francisco, CA, USA, Jun. 2008, pp. 395–403.

[11] F. Wang, J. Liu, and Y. Xiong, “Stable peers: Existence, importance, application in peer-to-peer live video streaming,” in *Proc. IEEE INFOCOM*, Phoenix, AZ, USA, Apr. 15–17, 2008, pp. 2038–2046.

[12] E. Lua, X. Zhou, J. Crowcroft, and P. Mieghem, “Scalable multicasting with network-aware geometric overlay,” *J. Comput. Commun. Archive*, vol. 31, no. 3, pp. 464–488, Feb. 2008.

[13] T. Do, K. Hua, and M. Tantaoui, “Robust video-on-demand streaming in peer-to-peer environments,” *Comput. Commun.*, vol. 31, no. 3, pp. 506–519, Feb. 2008.

[14] S. Banerjee, B. Bhattacharjee, and C. Kommareddy, “Scalable application layer multicast,” in *Proc. ACM SIGCOMM*, Aug. 2001, pp. 205–217.

[15] A. Lombardo, D. Reforgiato, and G. Schembra, “P2P and MPEG FGS encoding: A good recipe for multipoint video transmission on the internet,” *Int. J. Digit. Multimedia Broadcast.*, vol. 2009, pp. 453 471-1–453 471-21, Jan. 2009.

[16] L. Favalli, M. Folli, A. Lombardo, D. Reforgiato, and G. Schembra, “Design of a service platform for delay-sensitive video streaming applications based on multicast p2p and scalable MDC encoding,” *Comput. Commun.*, vol. 35, no. 18, pp. 2254–2263, Nov. 2012.

[17] V. N. Padmanabhan, H. J. Wang, and P. A. Chou, “Distributing streaming media content using cooperative networking,” in *Proc. NOSSDAV*, May 2002, pp. 177–186.

[18] V. K. Goyal, “Multiple description coding: Compression meets the network,” *IEEE Signal Process. Mag.*, vol. 18, no. 5, pp. 74–94, Sep. 2001.

[19] C. Yanghua, S. G. Rao, and Z. Hui, “A case for end system multicast,” in *Proc. ACM SIGMETRICS*, Santa Clara, CA, USA, 2000, pp. 1–12.

[20] Y. Chawathe, S. McCanne, and E. A. Brewer, “RMX: Reliable multicast for heterogeneous networks,” in *Proc. IEEE INFOCOM*, Tel Aviv, Israel, 2000, pp. 795–804.

[21] Y. Kim, D. Mazzocchi, and G. Tsudik, “Admission control in peer groups,” in *Proc. IEEE Int. Symp. NCA*, Apr. 2003, pp. 131–139.

[22] N. Saxena, G. Tsudik, and J. H. Yi, “Admission control in peer-to-peer: Design and performance evaluation,” in *Proc. 1st ACM Workshop Security Ad Hoc Sensor Netw.*, Fairfax, VA, USA, 2003, pp. 104–113.

[23] J. H. Møller, M. V. Pedersen, F. Fitzek, and T. Larsen, “Network coding for mobile devices-systematic binary random rateless codes,” in *Proc. IEEE ICC*, 2009, pp. 1–6.

[24] B. Ramesh, N. Savitha, and A. E. Manjunath, “Mobile applications in multimedia cloud computing,” *Int. J. Comput. Technol. Appl.*, vol. 4, no. 1, pp. 97–103, Jan./Feb. 2013.

[25] S. Wang, “Adaptive mobile cloud computing to enable rich mobile multimedia applications,” *IEEE Trans. Multimedia*, vol. 15, no. 4, pp. 870–883, Jun. 2013.

[26] G. Kemeni and J. L. Snell, *Finite Markov Chains*. Princeton, NJ, USA: Van Nostrand, 1960.

[27] G. Incarbone, A. Lombardo, D. Reforgiato, and G. Schembra, “A comprehensive platform to manage peer churn and bandwidth fluctuations in real-time multimedia P2P networks,” *J. Multimedia Tools Appl.*, vol. 63, no. 3, pp. 851–873, Apr. 2013.

[28] Y. Guo, K. Suh, J. Kurose, and D. Towsley, “P2Cast: Peer-to-peer patching scheme for VoD service,” in *Proc. 12th WWW Conf.*, May 2003, pp. 301–309.

[29] A. Lombardo, A. Masto, D. Reforgiato, and G. Schembra, “A dynamic jitter-controlled tree-based P2P network topology for multipoint multimedia applications,” *J. Interconnect. Netw.*, vol. 13, no. 1/2, pp. 1 250 003-1–1 250 003-19, Mar./Jun. 2012.

[30] T. Li, M. Chen, D.-M. Chiu, and M. Chen, “Queuing models for peer-to-peer systems,” in *Proc. 8th IPTPS*, Boston, MA, USA, Apr. 21, 2009, p. 4.

[31] G. Incarbone and G. Schembra, Maximizing the revenue of new P2P service providers for small high-interactive groups through an analytical tool for price decision, Univ. Catania, Catania, Italy, TR3.12. [Online]. Available: www.diit.unict.it/arti/TR/TR3_12.pdf

[32] R. W. Wolff, “Poisson arrivals see time averages,” *Oper. Res.*, vol. 30, no. 2, pp. 223–231, Mar./Apr. 1982.

[33] H. Qiu, Y. Li, J. Wu, and X. Gu, “Compensation buffer sizing for providing user-level QoS guarantee of media flows,” in *Proc. IEEE ICC*, Beijing, China, May 23–29, 2008, pp. 90–94.

[34] Y. J. Liang, N. Färber, and B. Girod, “Adaptive playout scheduling and loss concealment for voice communication over IP networks,” *IEEE Trans. Multimedia*, vol. 5, no. 4, pp. 532–543, Dec. 2003.

[35] A. P. Miettinen and J. K. Nurminen, “Energy efficiency of mobile clients in cloud computing,” in *Proc. 2nd USENIX Conf. Hot Topics Cloud Comput.*, Boston, MA, USA, Jun. 22–25, 2010, p. 4.

Giovanni Schembra received the degree in electrical engineering from the University of Catania, Catania, Italy, in 1991, the Master’s degree from CEFRIEL, Milan, Italy, in 1992, and the Ph.D. degree in electronics, computer science and telecommunications engineering. His Master’s thesis was on the analytical performance evaluation in an ATM network and the Ph.D. dissertation is on multimedia traffic modeling in a broadband network. He is currently an Associate Professor in telecommunications at the University of Catania.

His research interests are mainly concerned with software defined networks (SDNs), network functions virtualization (NFV), traffic modeling, and transmission of multimedia traffic in variable bandwidth wired/wireless environments.

Giuseppe Incarbone was born in Gela, Italy, in 1975. He received the degree in electronics engineering from the University of Catania with a thesis concerning the problem of videostreaming over a P2P framework with particular attention to Microsoft research Coopnet protocol, the Master’s degree in statistics from ETH Zurich with a thesis on t-tests for inference in robust regression, and the Ph.D. degree in mathematics for economic and financial decisions with a dissertation on cluster weighted models in 2013. He currently collaborates with the DIEEI, University of Catania, on projects regarding mobile clouds.

He is involved in the analitycal modelization of systems and network protocols. His research interests include the evaluation of the performances of P2P protocols for mediastreaming using both analytical models and simulations.

In March 2007, he won a scholarship for the study of P2P videostreaming systems and he took part in the research project PeeR-to-peer beyOnd FILE Sharing (PROFILES) partially supported by MIUR under the PRIN funding program, 2007–2008.